Metal-Nitroxyl Interactions. 46. EPR Spectra of Low-Spin Iron(III) Complexes of Spin-Labeled Tetraphenylporphyrins and Their Implications for the Interpretation of EPR Spectra of Spin-Labeled Cytochrome P450

Lee Fielding, Kundalika M. More, Gareth R. Eaton,* and Sandra S. Eaton

Contribution from the Departments of Chemistry, University of Denver, Denver, Colorado 80208, and University of Colorado at Denver, Denver, Colorado 80202. *Received September 3, 1985*

Abstract: Low-spin iron(III) complexes of seven spin-labeled tetraphenylporphyrins have been prepared. The spin labels were attached by amide or amide and ether linkages (three–eight bonds) to the ortho position of one phenyl ring. The axial ligands were imidazole and 1-methylimidazole. Computer simulations of the frozen solution EPR spectra were done with perturbation calculations and fourth-order frequency shift perturbation calculations. In frozen solution the complexes with amide linkages between the phenyl and nitroxyl rings adopted two conformations. The populations of the conformations were solvent-dependent. In one conformation the values of the electron–electron spin–spin coupling constants, J, were between ± 0.22 and ± 0.28 cm^{-1}. Addition of a CH_2 group between the amide and the nitroxyl caused J to decrease by a factor of 3–7. The spin–spin interaction in the second conformation was much weaker than in the first conformation. Resolved spin–spin splitting was not observed for this conformation although the line widths for the nitroxyl signal in frozen solution were increased due to interaction with the iron. Broadening of the nitroxyl signal in frozen solution was also observed for complexes with longer ether linkages between the phenyl ring and the nitroxyl. In fluid solution the integrated intensities of the nitroxyl signals indicated that the observed spectra were due only to the conformations with weak spin–spin interaction. The EPR spectra, reported by other authors, of two spin labels coordinated to ferric cytochrome P450 were analyzed with the computer programs developed for the iron porphyrin model systems. The values of J for the two complexes were ± 0.03 and $\pm|>0.4|$ cm^{-1}. These spectra indicate that electron–electron exchange interaction as well as dipolar interaction must be considered in analyzing the spectra of spin-labeled biomolecules.

Introduction

Isocyanides, pyridines, and alkylamines bind to the heme in ferric cytochrome P450 to give 6-coordinate low-spin complexes (type II ligands).[1,2] Spin-labeled isocyanides,[3-9] pyridines,[10-12] and alkylamines[6,13] have been coordinated to ferric cytochrome P450. In the interpretation of the EPR spectra of these complexes it was assumed that there was only dipolar interaction between the unpaired electron on the iron and the unpaired electron on the nitroxyl radical. Although the frozen solution EPR spectrum of one spin-labeled complex of cytochrome P450 has been shown to be consistent with dipolar interaction between the two unpaired electrons,[12] spectra of other spin-labeled cytochrome P450 samples in frozen solution have been published, without interpretation, that do not appear to be consistent with dipolar interaction alone.[5,6,13] We have previously shown that both exchange and dipolar contributions to electron–electron spin–spin interaction must be considered for a variety of spin-labeled complexes of Cu(II),[14-17] Ag(II),[18-20] VO(IV),[17,18,21] and Mn(II).[22,23] It was therefore of interest to analyze the spin–spin interactions that give rise to the EPR spectra in spin-labeled Fe(III) complexes.

One difficulty in analyzing the results for the cytochrome P450 complexes was that no data were available for model compounds of known structure containing low-spin iron(III) and nitroxyl radicals. There were therefore no EPR spectra with which to compare the spectra of the spin-labeled cytochrome P450 samples and no calibration of the models proposed for obtaining estimates of the distance between the iron and the nitroxyl.

We have therefore prepared a series of low-spin iron(III) complexes of spin-labeled porphyrins. The EPR spectra of the imidazole and 1-methylimidazole complexes of iron porphyrins I–VII were studied in fluid solution and frozen solution.[24] A brief report of the spectra of the imidazole and 1-methylimidazole complexes of II has been published.[25]

Experimental Section

Physical Measurements. Visible spectra were obtained on chloroform solutions on a Beckman Acta V spectrophotometer or a Cary 14 with the OLIS modification.[26] Wavelengths of peak maxima are reported below

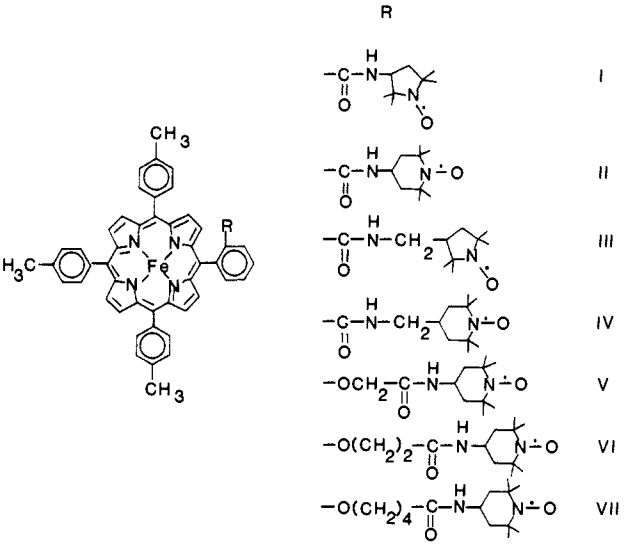

in nanometers and log ϵ is given in parentheses. Infrared spectra were obtained on halocarbon mulls or KBr pellets on a Perkin-Elmer 283B

* Address correspondence to this author at the University of Denver.

(1) Lemberg, R.; Barrett, J. "Cytochromes": Academic Press: New York, 1973.
(2) Hill, H. A. O.; Roder, A.; Williams, R. J. P. *Struct. Bonding (Berlin)* **1970**, *8*, 123.
(3) Reichman, L. M.; Annaev, B.; Rozantsev, E. G. *Biochim. Biophys. Acta* **1972**, *263*, 41.
(4) Raikhman, L. M.; Annayev, B.; Mamedniyazov, O. N.; Rozantsev, E. G. *Biofizika* **1973**, *18*, 228 (p 235 in translation).
(5) Pirrwitz, J.; Rein, H.; Lassmann, G.; Janig, G. R.; Pecar, S.; Ruckpaul, K. *FEBS Lett.* **1979**, *101*, 195.
(6) Pirrwitz, J.; Lassman, G.; Rein, H.; Janig, G.-R.; Pecar, S.; Ruckpaul, K. *Acta Biol. Med. Germ.* **1979**, *38*, 235.
(7) Schwarz, D.; Pirrwitz, J.; Rein, H.; Ruckpaul, K. *J. Magn. Reson.* **1982**, *47*, 375.
(8) Schwarz, D.; Pirrwitz, J.; Ruckpaul, K. *Arch. Biochem. Biophys.* **1982**, *216*, 322.
(9) Schwarz, D.; Pirrwitz, J.; Rein, H.; Ruckpaul, K. *Biomed. Biochim. Acta* **1984**, *43*, 295.
(10) Griffin, B. W.; Smith, S. M.; Peterson, J. A. *Arch. Biochem. Biophys.* **1974**, *160*, 323.

0002-7863/86/1508-0618$01.50/0

spectrometer. NMR spectra were recorded on deuteriochloroform solutions on a Chemagnetics A200. Chemical shifts are reported relative to tetramethylsilane. X-band EPR spectra were obtained on a Varian E9 interfaced to a Varian 620/L103 or an IBM CS9000. The spectrometer used for the Q-band measurements has been described.[27] The spectra of the complexes in the *S* conformation (defined below) were not concentration-dependent between 0.1 and 3.0 mM. Most of the data were obtained at 0.5–1.0 mM for frozen solutions and 0.5–2.0 mM for fluid solutions. The lines in the spectra of most of the complexes were sufficiently broad that the line widths were unchanged by removal of oxygen. Spectra discussed below were obtained on samples that were not degassed unless otherwise noted. All spectra were obtained at microwave powers well below saturation and at modulation amplitudes that did not cause distortion of the line shapes. Elemental analyses were performed by Spang Microanalytical Laboratory. Mass spectral determinations were obtained by fast atom bombardment at the Midwest Center for Mass Spectrometry.

Quantitation of the EPR signals was done by comparison of the double integrals with double integrals for solutions of known concentration of 2,2,6,6-tetramethylpiperidin-1-yl or 4-oxo-2,2,6,6-tetramethylpiperidin-1-yl in the same solvent and sample tube. Throughout the ensuing text integration and integrals refers to double integrals of the first derivative spectra.

Preparation of Compounds. The reactions involving acid chlorides were performed under a dry nitrogen atmosphere to minimize hydrolysis. Other reactions were performed in air, unless otherwise noted.

5-(2-(Carboxymethoxy)phenyl)-10,15,20-tri-*p*-tolylporphyrin (H_2(O-CH_2COOH-TTP)). Bromoacetic acid, 0.14 g (0.020 mmol), in 5 mL of DMF was slowly added (1.5 h) to a solution of 274 mg of 5-(2-hydroxy)-10,15,20-tri-*p*-tolylporphyrin[28] and 0.21 g of powdered KOH in 20 mL of DMF. The solution was stirred at room temperature for 25 h and then the DMF was removed. The residue was dissolved in 100 mL of chloroform, washed with dilute HCl, water, and 2% sodium acetate solution, and chromatographed on 174 g of silica gel. Unreacted porphyrin was eluted with chloroform. The product was eluted with 9:1 chloroform/methanol and recrystallized from chloroform/heptane. IR 1620 cm^{-1} (CO); vis 644 (3.66), 590 (3.71), 551 (3.89), 516 (4.22), 420 (5.67); NMR δ −2.72 (s, 2 H, NH), 2.69 (s, 9 H, *p*-CH_3), 4.42 (s, 2 H, OCH_2), 4.76 (d, 1 H, *m*-H on ortho-substituted phenyl), 7.55 (d, 6 H, *m*-H on tolyl rings), 7.79 (m, 1 H, ortho H on ortho-substituted phenyl), 8.09 (d, 6 H, ortho H on tolyl rings), 8.82 (m, 8 H, pyrrole H).

Iron(III) 5-(2-Carboxyphenyl)-10,15,20-tri-*p*-tolylporphyrin Chloride (Fe(COOH-TTP)Cl). 5-(2-Carboxyphenyl)-10,15,20-tri-*p*-tolylporphyrin[29] (0.080 g, 0.11 mmol) was dissolved in glacial acetic acid (100 mL) under nitrogen and heated to 85 °C. Pyridine (1.5 mL) and $FeSO_4 \cdot 7H_2O$ (1.5 mL of saturated aqueous solution) were added and heating was continued for 30 min. The solution was cooled and 100 mL of H_2O was added. The iron porphyrin was collected by filtration, washed with H_2O, and chromatographed on silica gel in $CHCl_3$/MeOH (98.5:1.5). The eluant was shaken with 2 M aqueous HCl and the solvent was removed. The product was recrystallized from CH_2Cl_2/hexane. Yield 0.071 g, 82%; IR 1720 (CO) cm^{-1}; vis 697 (3.44), 662 sh (3.39), 578 (3.56), 512 (4.11), 418 (4.97), 382 (4.74).

Iron(III) 5-(2-(Carboxymethoxy)phenyl)-10,15,20-tri-*p*-tolylporphyrin Chloride (Fe(OCH$_2$COOH-TTP)Cl). H_2(OCH$_2$COOH-TPP), 0.23 g, was dissolved in 200 mL of acetic acid and 4 mL of pyridine under nitrogen. The solution was heated to 90 °C, 4 mL of saturated aqueous $FeSO_4$ was added, and heating was continued for 15 min. The color of the solution changed from green to dark purple. The solution was cooled and poured into 1 L of cold water. The precipitate was collected by filtration, air-dried, and redissolved in 50 mL chloroform. The solution was chromatographed on 145 g of silica gel. Elution with 4% methanol in chloroform caused the product to move down the column slightly ahead of unreacted porphyrin (42 mg). The solvent was removed in vacuum. The residue was dissolved in chloroform and the solution was washed with 0.1 M HCl. The iron porphyrin was recrystallized from chloroform/heptane. Yield 134 mg; IR 1620 (CO) cm^{-1}; vis 675 (3.52), 650 sh (3.48), 577 (3.57), 506 (4.14), 416 (5.00), 379 (4.76).

Iron(III) 5-(2-(((2,2,5,5-Tetramethyl-1-oxypyrrolidin-3-yl)amido)-carbonyl)phenyl)-10,15,20-tri-*p*-tolylporphyrin Chloride (I-Cl). Oxalyl chloride (26 mmol), 3.0 g, was added to a solution of 0.37 g of Fe(COOH-TTP)Cl in 200 mL of benzene. After 4 h the solvent was removed and the residue was dried in vacuum for 3 h and redissolved in 250 mL of dry THF. Pyridine, 1 g, and 72 mg of 3-amino-2,2,5,5-tetramethyl-1-oxypyrrolidin-3-yl (0.46 mmol) were added and the solution was refluxed under nitrogen for 12 h. The solvent was removed and the residue was dried in vacuum for 1 h before it was dissolved in 120 mL of chloroform. The chloroform solution was washed twice with 0.01 M HCl, twice with 0.01 M KOH, once with 0.02 M HCl, and chromatographed on 75 g of silica gel. The product that was eluted with 2% methanol in chloroform (0.31 g) was recrystallized from chloroform/heptane. It was redissolved in 50 mL of chloroform, shaken with 0.1 M KOH, and rechromatographed on 81 g of alumina. The product was eluted with chloroform, and the solution was shaken with 0.03 M HCl. The product was precipitated with heptane, collected by filtration, and dried to constant weight in vacuum. Yield 26%, IR 1670 cm^{-1} (CO); vis 694 (3.50), 660 sh (3.44), 575 (3.59), 511 (4.13), 418 (5.01), 382 (4.77). Anal. Calcd for $C_{56}H_{49}N_6O_2FeCl$: C, 72.37, H, 5.31, N, 9.04, Cl, 3.81. Found: C, 72.65, H, 5.68, N, 8.85, Cl, 4.03.

Iron(III) 5-(2-(((2,2,6,6-Tetramethyl-1-oxypiperidin-4-yl)amido)-carbonyl)phenyl)-10,15,20-tri-*p*-tolylporphyrin μ-Oxo-Bridged Dimer ((II)$_2$O). This complex was prepared from Fe(COOH-TTP)Cl and 2,2,6,6-tetramethyl-1-oxypiperidin-4-yl by the procedure reported for I-Cl except that it was isolated as the μ-oxo bridged dimer which was prepared by allowing a solution of II-OH to stand overnight before it was chromatographed on alumina. Yield: 27%. IR: 1660 cm^{-1} (CO). VIS: 614 (3.82), 574 (4.02), 414 (5.05), 320 (4.51). Anal. Calcd for $C_{114}H_{102}N_{12}O_5Fe \cdot 0.25CHCl_3$: C, 73.71, H, 5.54, N, 9.03, Cl, 1.43. Found: C, 73.84, H, 5.79, N, 9.13, Cl, 1.52.

Iron(III) 5-(2-((((2,2,5,5-Tetramethyl-1-oxypyrrolidin-3-yl)-methylene)amido)carbonyl)phenyl)-10,15,20-tri-*p*-tolylporphyrin Chloride (III-Cl). Fe(COOH-TTP)Cl (0.079 g, 0.10 mmol) was dissolved in dry benzene (50 mL). Oxalyl chloride (1.13 g, 10 mmol) was added and the solution was stirred at room temperatue for 2 h. The benzene was removed under vacuum and the residue was dried under vacuum for 2 h. The residue was dissolved in dry THF (75 mL) and 3-(aminomethyl)-2,2,5,5-tetramethyl-1-oxypyrrolidinyl[30] (17 mg, 0.1 mmol) was added. The solution was refluxed gently for 3 h and then the solvent was removed in vacuum. The product was chromatographed on silica gel in $CHCl_3$/MeOH (98.5:1.5). The solution was washed 3 times with 0.1 M HCl. The solvent was removed and the product was recrystallized from $CHCl_3$/hexane. Yield 67%; IR 1660 (CO), 3410 (NH) cm^{-1}; vis 692 (3.54), 655 (3.46), 575 (3.61), 510 (4.15), 419 (5.03), 380 (4.75), 350 sh (4.60). Anal. Calcd for $C_{57}H_{51}N_6O_2FeCl$: C, 72.58, H, 5.45, N, 8.90, Cl, 3.76. Found: C, 72.39, H, 5.58, N, 9.02, Cl, 3.69.

Iron(III) 5-(2-((((2,2,6,6-Tetramethyl-1-oxypiperidin-4-yl)-methylene)amido)carbonyl)phenyl)-10,15,20-tri-*p*-tolylporphyrin Chloride (IV-Cl). The complex was prepared from Fe(COOH-TTP)Cl and 4-(aminomethyl)-2,2,6,6-tetramethyl-1-oxy-piperidin-4-yl[31] by the method

(11) Ruf, H. H.; Nastainczyk, W. *Eur. J. Biochem.* **1976**, *66*, 139.
(12) Mock, D. M.; Bruno, G. V.; Griffin, B. W.; Peterson, J. A. *J. Biol. Chem.* **1982**, *257*, 5372.
(13) Pirrwitz, J.; Lassman, G.; Rein, H.; Ristau, O.; Janig, G. R.; Ruckpaul, K. *FEBS Lett.* **1977**, *83*, 15.
(14) Eaton, S. S.; More, K. M.; Sawant, B. M.; Boymel, P. M.; Eaton, G. R. *J. Magn. Reson.* **1983**, *52*, 435.
(15) More, K. M.; Eaton, G. R.; Eaton, S. S. *Can. J. Chem.* **1982**, *60*, 1392.
(16) Damoder, R.; More, K. M.; Eaton, G. R.; Eaton, S. S. *J. Am. Chem. Soc.* **1983**, *105*, 2147.
(17) More, K. M.; Eaton, G. R.; Eaton, S. S. *J. Magn. Reson.* **1984**, *59*, 497.
(18) More, K. M.; Eaton, S. S.; Eaton, G. R. *J. Am. Chem. Soc.* **1981**, *103*, 1087.
(19) More, K. M.; Eaton, G. R.; Eaton, S. S. *Inorg. Chem.* **1984**, *23*, 4084.
(20) Damoder, R.; More, K. M.; Eaton, G. R.; Eaton, S. S. *Inorg. Chem.* **1983**, *22*, 3738.
(21) Damoder, R.; More, K. M.; Eaton, G. R.; Eaton, S. S. *Inorg. Chem.* **1983**, *22*, 2836.
(22) More, J. K.; More, K. M.; Eaton, G. R.; Eaton, S. S. *J. Am. Chem. Soc.* **1984**, *106*, 5395.
(23) More, K. M.; Eaton, G. R.; Eaton, S. S. *J. Magn. Reson.* **1985**, *63*, 151.
(24) Abbreviations: P, porphyrin dianion; Im, imidazole; MeIm, 1-methylimidazole; pip, piperidine.
(25) Eaton, S. S.; Fielding, L.; More, K. M.; Damoder, R.; Eaton, G. R. *Bull. Magn. Reson.* **1983**, *5*, 176.
(26) The On-Line Instruments System (OLIS) 3920 modification replaces the Cary 14 electronics with stepper motors for the slit and monochromator and controls the system with a Zenith Z-100 microcomputer with 13 bit A/D and D/A converters.
(27) Eaton, S. S.; More, K. M.; DuBois, D. L.; Boymel, P. M.; Eaton, G. R. *J. Magn. Reson.* **1980**, *41*, 150.
(28) Little, R. G.; Anton, J. A.; Loach, P. A.; Ibers, J. *J. Heterocycl. Chem.* **1975**, *12*, 343.
(29) More, K. M.; Sawant, B. M.; Eaton, G. R.; Eaton, S. S. *Inorg. Chem.* **1981**, *20*, 3354.
(30) Boymel, P. M.; Braden, G. A.; Eaton, G. R.; Eaton, S. S. *Inorg. Chem.* **1980**, *19*, 735.

used to prepare III-Cl. Yield 60%; IR 1660 (CO), 3410 (NH) cm^{-1}; vis 694 (3.57), 655 (3.53), 578 (3.66), 511 (4.15), 420 (4.99), 381 (4.71), 354 sh (4.57). Anal. Calcd for $C_{58}H_{53}N_6O_2FeCl$: C, 72.77, H, 5.58, N, 8.77, Cl, 3.70. Found: C, 72.04, H, 5.68, N, 8.60, Cl, 3.68. The low carbon analysis is attributed to water retained in the crystals despite prolonged drying in vacuum. About $^1/_3$ mol of water per mol of iron porphyrin would account for the discrepancy between the calculated and observed analyses.

Iron(III) 5-(2-((((2,2,6,6-Tetramethyl-1-oxypiperidin-4-yl)amido)carbonyl)methoxy)phenyl)-10,15,20-tri-*p*-tolylporphyrin Chloride (V-Cl). This complex was prepared from $Fe(OCH_2COOH)Cl$ and 2,2,6,6-tetramethyl-1-oxypiperidin-4-yl by the procedure reported for I-Cl. Yield 44%; IR 1690 cm^{-1} (CO); vis 692 (3.55), 654 (3.47), 576 (3.55), 511 (4.16), 419 (5.03), 380 (4.78); mass spectrum, m/z (M − Cl) 937.35. Anal. Calcd for $C_{58}H_{53}N_6O_3FeCl$: C, 71.57, H, 5.49, N, 8.63, Cl, 3.64. Found: C, 71.43, H, 5.63, N, 8.69, Cl, 3.54.

Iron(III) 5-(2-((((2,2,6,6-Tetramethyl-1-oxypiperidin-4-yl)amido)carbonyl)ethoxy)phenyl)-10,15,20-tri-*p*-tolylporphyrin Chloride (VI-Cl). The complex was prepared from iron(III) 5-(2-(2-carboxyethoxy)-phenyl)-10,15,20-tri-*p*-tolylporphyrin chloride[32] and 4-amino-2,2,6,6-tetramethyl-1-oxy-piperidin-4-yl by the method reported for III-Cl. Yield 63%; IR 1670 (CO), 3390 (NH) cm^{-1}; vis 694 (3.45), 657 (3.39), 579 (3.50), 512 (4.10), 418 (4.98), 383 (4.74), 350 sh (4.53); mass spectrum, m/z (M − Cl) 951.37. Anal. Calcd for $C_{59}H_{55}N_6O_3FeCl$: C, 71.77, H, 5.61, N, 8.51, Cl, 3.59. Found: 71.57, H, 5.74, N, 8.60, Cl, 3.68.

Iron(III) 5-(2-((((2,2,6,6-Tetramethyl-1-oxypiperidin-4-yl)amido)carbonyl)butoxy)phenyl)-10,15,20-tri-*p*-tolylporphyrin Chloride (VII-Cl). The complex was prepared from iron(III) 5-(2-(4-carboxybutoxy)-phenyl)-10,15,20-tri-*p*-tolylporphyrin chloride[32] and 4-amino-2,2,6,6-tetramethyl-1-oxy-piperidin-4-yl by the procedure reported for III-Cl. Yield 65%; IR 1660 (CO), 3350 (NH) cm^{-1}; vis 694 (3.47), 660 (3.39), 579 (3.51), 512 (412), 418 (4.99), 385 (4.76), 351 sh (4.54); mass spectrum, m/z (M − Cl) 979.40. Anal. Calcd for $C_{61}H_{59}N_6O_3FeCl$: C, 72.15, H, 5.86, N, 8.27, Cl, 3.49. Found: C, 72.30, H, 6.00, N, 8.11, Cl, 3.48.

Preparation of Solutions for EPR Studies. $Fe(P)(Im)_2^+$ and $Fe(P)(MeIm)_2^+$. A solution of spin-labeled porphyrin chloride or μ-oxo-bridged dimer in toluene solution (1–5 mM) was shaken with 0.05 M HCl to convert all μ-oxo-bridged dimer to Fe(P)Cl. The phases were separated and a 10-fold, or greater, excess of imidazole (in chloroform solution) or 1-methylimidazole was added to the organic phase. The rapid color change from brown to bright red-orange was characteristic of the formation of the low-spin 6-coordinate complexes. The solutions were then diluted to the desired concentration with solvent containing imidazole or 1-methylimidazole. EPR spectra and visible spectra indicated that the conversion from 5-coordinate high-spin porphyrin to 6-coordinate low-spin porphyrin was quantitative. Most of the imidazole complexes of the spin-labeled iron porphyrins were not sufficiently soluble in toluene to permit EPR measurements, unless about 10% chloroform was included in the solvent mixture.

$Fe(P)(pip)_2$. Fe(P)Cl was dissolved in piperidine or 1:1 toluene/piperidine to give approximately 1 mM solutions. At this concentration the visible spectra and EPR spectra indicated that >95% of the iron porphyrin was converted to the low-spin ($S = 0$) Fe(II) form.[33] As the iron porphyrin concentration was decreased below 1 mM, while maintaining constant piperidine concentration, the frozen solution EPR spectra showed increasing concentrations of a species with $g \sim 4.3$ and the visible spectra showed a broad sloping base line, rising toward higher energies. Thus there appear to be complications in the equilibria at low concentrations, although the spectra indicated a single component at higher concentrations. Therefore the spectra of $Fe(P)(pip)_2$ cited in this paper were obtained at concentrations greater than 1 mM.

Computer Simulations. Since 98% of naturally occurring iron has nuclear spin $I = 0$ and since low-spin iron(III) has $S = ^1/_2$, the Hamiltonian for the spin system is given by eq 1 where 1 and 2 refer to the

$$\mathcal{H} = \beta S_1 \cdot g_1 \cdot H + \beta S_2 \cdot g_2 \cdot H + A_2 \cdot I_2 \cdot S_2 + J S_1 \cdot S_2 + \mathcal{H}_{\text{dipolar}} \quad (1)$$

unpaired electrons on iron(III) and nitroxyl, respectively, J is the electron–electron coupling constant, A_2 is the electron–nuclear coupling constant between the nitroxyl unpaired electron and the nitroxyl nitrogen nuclear spin, and other symbols have their usual meanings. The computer program MENO[14] is based on a perturbation solution to eq 1. However, for several of the complexes examined, the value of J was approximately equal to the observing magnetic field, which can result in large values of the perturbation correction terms. Therefore there was concern that the simulated spectra might not be reliable. A second program (METNO) was written to solve eq 1 using Belford's fourth-order frequency shift perturbation method.[34,35] Since the line widths in the spectra of the complexes with $J > 0.02$ cm^{-1} were greater than the nitroxyl nitrogen hyperfine splitting, the hyperfine splitting was not included in the calculation. The field at which the diagonalization was performed was varied to check the accuracy of the results. The simulated spectra obtained from the two programs were in good agreement.

The g values used in the simulations were the following: Fe(III), $g_x = 1.515$–1.535, $g_y = 2.25$–2.27, $g_z = 2.91$–2.93; nitroxyl, $g_x = 2.0089$, $g_y = 2.0062$, $g_z = 2.0027$.[14] The nitroxyl hyperfine splittings used in the calculations with MENO were A_x, A_y 5×10^{-4} cm^{-1}, and A_z 32×10^{-4} cm^{-1}.[14] The simulations were insensitive to small variations in the nitroxyl g and A values. For the complexes with J greater than 0.2 cm^{-1} the dipolar interaction was small compared with the exchange interaction. For these complexes satisfactory simulated spectra were obtained with r greater than or equal to 7 Å. Smaller values of r gave spectra that were not consistent with the experimental spectra. For the complexes with smaller values of J the line widths were so large that the anisotropy in the spin–spin interaction was obscured. Therefore in both types of spectra there was uncertainty in the parameters that define the orientation of the interspin vector relative to the g axes of iron(III). Satisfactory simulated spectra were obtained for either positive or negative values of J.

Results and Discussion

The spin-labeled iron porphyrins were prepared by reaction of Fe(II) with ortho-substituted porphyrins followed by attachment of the spin label because attempts to react Fe(II) with spin-labeled porphyrins resulted in reduction of the nitroxyl radical. The complexes were isolated and characterized as the high-spin iron(III) porphyrin chlorides (Fe(P)Cl) or μ-oxo-bridged dimers ($(Fe(P))_2O$). To check that the spin-labeling was quantitative, the $Fe(P)(pip)_2$ complexes were examined in which the iron is diamagnetic Fe(II). Integration of the spectra confirmed the presence of 1 mol of nitroxyl per mol of iron porphyrin. Solutions of $Fe(P)(Im)_2^+$ and $Fe(P)(MeIm)_2^+$ were prepared by dissolving the iron porphyrin chlorides in solvent containing excess imidazole or 1-methylimidazole, respectively. These ligands cause complete conversion to low-spin iron(III). Solutions of Fe(P) in pyridine were mixtures of high-spin and low-spin iron(III). Addition of 2-methylimidazole to solutions of Fe(P)Cl caused formation of μ-oxo-bridged dimer. Therefore only the complexes with imidazole and 1-methylimidazole were studied. The EPR spectra contained no evidence for aggregation of the $Fe(P)(Im)_2^+$ complexes, which is consistent with NMR studies.[36]

EPR Spectra in Frozen Solution. The typical low-spin iron(III) EPR spectrum obtained for $FeTTP(Im)_2^+$ in frozen solution (−180 °C) is shown in Figure 1A. The simulated spectrum was obtained with g values of 1.52, 2.27, and 2.91 and line widths of 60–200 G. The EPR spectra of $I\text{-}(MeIm)_2^+$ and $I\text{-}(Im)_2^+$ obtained under similar conditions are shown in Figure 1B,C. The spectra for the two complexes were similar although the line widths were greater for the imidazole complex than for the 1-methylimidazole complex. Both spectra were markedly different from the spectrum of $FeTTP(Im)_2^+$. The simulated spectra were obtained with $r = 7$ Å and $|J| = 0.28$ and 0.22 cm^{-1}, respectively. This magnitude of J was sufficiently large relative to the difference between the nitroxyl g values (~2) and the iron g_x (1.52) and g_y (2.27) values to give rise to turning points at the average g values, 1.76 and 2.14. The exchange interaction was not strong enough to fully average the larger difference between the iron g_x and nitroxyl signal so partially averaged, but resolved, signals were observed at $g \sim 2.61$ and 2.32. The sharp signal at $g \sim 2$, corresponded to about 10% of the nitroxyl intensity. There also were weak signals at the g values observed for $FeTTP(Im)_2^+$. These signals are assigned to a second conformation (W) of the complexes in which the spin–spin interaction is much smaller than in the conformation (S) that

(31) Shapiro, A. B.; Bogach, L. S.; Chumakov, V. M.; Kropacheva, A. A.; Suskina, V. I.; Rozantsev, E. G. *Izv. Akad. Nauk SSSR Ser. Khim.* **1975**, 2077. More K. M.; Eaton, G. R.; Eaton, S. S., unpublished results.
(32) More, K. M.; Eaton, G. R.; Eaton, S. S. *Inorg. Chem.* **1985**, *24*, 3698.
(33) Gaudio, J. D.; LaMar, G. N. *J. Am. Chem. Soc.* **1978**, *100*, 1112.
(34) Belford, R. L.; Davis, P. H.; Belford, G. G.; Lenhardt, T. M. *ACS Symp. Ser.* **1974**, *No. 5*, 40.
(35) Scullane, M. I.; White, L. K.; Chasteen, N. D. *J. Magn. Reson.* **1982**, *47*, 383.
(36) Goff, H. M. *J. Am. Chem. Soc.* **1981**, *103*, 3714.

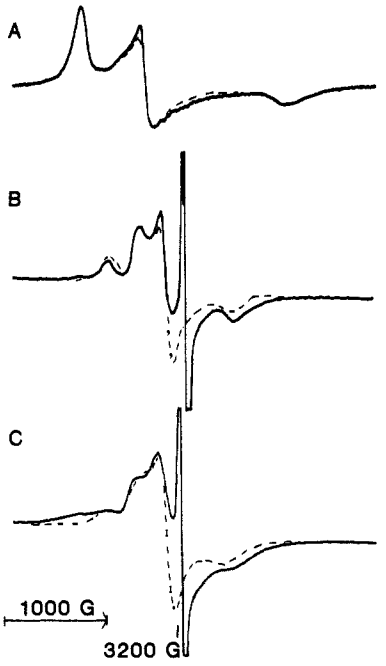

Figure 1. 4000-G scans of the X-band (9.10 GHz) EPR spectra at −180 °C of (A) 2 mM FeTTP(Im)$_2^+$, (B) 0.7 mM I-(MeIm)$_2^+$, and (C) 1.0 mM I-(Im)$_2^+$ in toluene/chloroform glasses. The modulation amplitudes were 5–10 G and the microwave power was 50–100 mW. The dashed lines denote the simulations in regions where the simulated spectra do not overlay the experimental curves. For the spectra of the spin-labeled complexes, the simulations included only the S conformation.

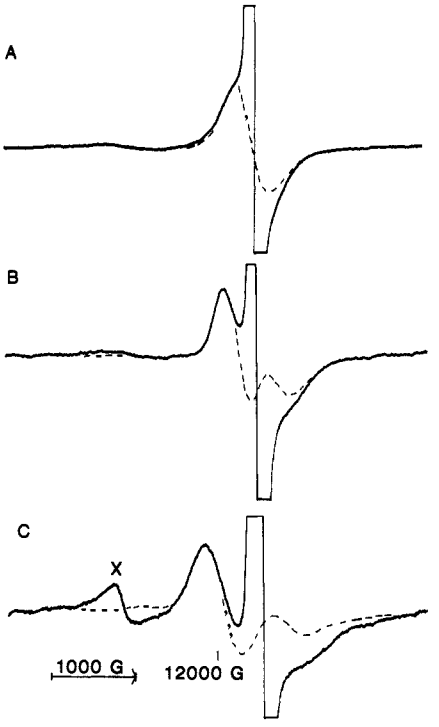

Figure 2. 5000-G scans of the Q-band (35 GHz) EPR spectra at −180 °C for (A) 3 mM IV-(Im)$_2^+$, (B) 3 mM III-(Im)$_2^+$, and (C) 3 mM IV-(MeIm)$_2^+$. The spectra were obtained with 5-G modulation amplitude and 148-mW microwave power. The dotted lines denote the simulated spectra for the S conformation. The peak marked with the X is the g = 2.26 signal for the low-spin Fe(III) in the W conformation.

gave $J \sim \pm 0.25$ cm^{-1}. The population of conformation W was determined by integration of 200-G scans centered at 3250 G ($g \sim 2$) and from the amplitude of the low-spin iron signal at g = 2.91. Due to variations in the line widths of the iron signals, there was greater uncertainty in the latter values than in the former, although the two were in general agreement. The populations of conformation W given in Table I were based on the integrations of the weakly interacting nitroxyl signals.

EPR spectra of II-(Im)$_2^+$ and II-(MeIm)$_2^+$ in frozen solution also showed the presence of two conformations that differed in the magnitude of the spin–spin interaction. The populations of conformation W were greater for these complexes than for the complexes of I. Overlap of the iron signals from conformation W with the signals from conformation S caused greater uncertainty in the values of J for these complexes than for the complexes of I. Substantial populations of conformation W (30–60%) were also observed for the complexes of III and IV. Q-band spectra were obtained for the complexes of I–IV. The line widths in the spectra of the complexes of I and II were larger than in the X-band spectra and the resolution of the spectra was not improved. The values of J obtained from the simulations of the Q-band spectra were consistent with the values obtained at X-band. For the complexes of III and IV, the Q-band spectra showed the nitroxyl signals for conformation S without overlap with the iron signals from conformation W. As the value of J increased, the splitting of the nitroxyl lines increased, and intensity spread to lower and higher field (Figure 2).

The values of J for the complexes of I and II (Table I) were between ±0.22 and ±0.28 cm^{-1}, which indicated that the spin–spin interaction was not strongly dependent on the size of the nitroxyl ring when the amide bond was attached directly to the nitroxyl ring. However, in the complexes of III and IV which have a CH_2 group between the nitroxyl and the amide linkage, the values of J were dependent on the axial ligand (Im or MeIm) and on the size of the nitroxyl ring. It has been shown previously that "W-plan" conformations of saturated linkages between metals and nitroxyls give rise to substantially larger exchange interactions than other conformations.[15] The size of the nitroxyl ring and the presence or absence of a methyl group on the imidazole could influence the steric interactions that determine the conformation of the CH_2 group and thereby cause changes in the values of J. Comparison of the values of J for the complexes of I and II with the values for the complexes of III and IV indicated that addition of the CH_2 group to the porphyrin–nitroxyl linkage caused the value of J to decrease by factors of 3–10. These decreases are similar to those observed in complexes in which the spin delocalization had larger contributions from σ orbitals than from π orbitals.[37]

The EPR spectra of the imidazole and 1-methylimidazole complexes of V to VII were superpositions of the spectra for low-spin iron(III) and nitroxyl radicals. The nitroxyl lines were broadened by interaction with the iron, but the spin–spin splitting was not resolved. Integration of 200-G scans centered at 3250 G indicated that the sharp nitroxyl signals accounted for 100% of the expected nitroxyl intensity. These spectra resembled those obtained for conformation W in the complexes of I to IV and so the spectra will be compared with those of conformation W, although different conformations are likely to occur for the ether linkages than for the amide linkages.

Possible Structures for Conformations W and S. Two conformations have previously been observed for the copper(II) and silver(II) analogues of II. In toluene or chloroform solution strong spin–spin interaction was observed, but in pyridine solution the value of J was approximately zero.[18,29] In frozen solution the metal–nitroxyl interspin distance was found to be about 2 Å longer for the conformation that gave the smaller value of J than for the conformation that gave the larger value of J.[14,19] It was therefore proposed that changes in the conformation of the metal–nitroxyl linkage influenced the value of J. Comparison of the values of J for a series of ortho-, meta-, and para-substituted spin-labeled copper porphyrins led to the suggestion that the strong spin–spin interaction in complexes with an amide linkage on the ortho carbon might be due to overlap of the orbitals on the carbonyl oxygen with the porphyrin π-orbitals.[29] Thus it was proposed that the carbonyl group was close to the porphyrin plane for the confor-

(37) More, J. K.; More, K. M.; Eaton, G. R.; Eaton, S. S. *Inorg. Chem.* **182**, *21*, 2455.

Table I. EPR Spectra in Frozen Solution at −180 °C

porphyrin	% conformation W: toluene[a]	% conformation W: $CHCl_3$	d_1/d[c]	rel amp[d]	J,[b] cm^{-1}
I-$(Im)_2^+$	7	8	0.50	0.38	±0.22
I-$(MeIm)_2^+$	10	15	0.50	0.42	±0.28
II-$(Im)_2^+$	20	44	0.68	0.25	±0.25
II-$(MeIm)_2^+$	40	78	0.70	0.37	±0.28
III-$(Im)_2^+$	50	65	0.51	0.57	±0.05
III-$(MeIm)_2^+$	60	100	0.51	0.53	±0.05
IV-$(Im)_2^+$	30	40	0.61	0.48	±0.025
IV-$(MeIm)_2^+$	50	65	0.55	0.66	±0.10
V-$(Im)_2^+$			0.53	0.81	
V-$(MeIm)_2^+$			0.56	0.81	
VI-$(Im)_2^+$			0.51	0.82	
VI-$(MeIm)_2^+$			0.51	0.78	
VII-$(Im)_2^+$			0.50	0.79	
VII-$(MeIm)_2^+$			0.51	0.91	

[a] 9:1 toluene/$CHCl_3$ was used for the imidazole adducts. [b] Electron–electron coupling constant for conformation S. [c] Ratio of height of central line to low- and high-field lines of nitroxyl signal for conformation W (see ref 40). [d] Ratio of amplitude of nitroxyl signal for conformation W to that expected in the absence of spin–spin interaction.

mation with the larger value of J and further from the porphyrin plane for the conformation with the smaller value of J. The observation of two conformations of the low-spin iron(III) complexes with substantially different values of J raises the possibility that these two conformations might be similar to those observed previously for Cu(II) and Ag(II).

^{13}C and ^1H NMR studies of Fe(P)$(Im)_2^+$ complexes have shown that there is substantial unpaired spin density on the pyrrole carbons[36] and hydrogens[38] and little spin density on the meso carbons.[36] Consequently overlap of the orbitals on the carbonyl oxygen with orbitals on the pyrrole carbons might provide a pathway for spin–spin interaction between the iron and the nitroxyl unpaired electrons. It is therefore proposed that in conformation S the carbonyl oxygen is sufficiently close to the porphyrin pyrrole ring to permit overlap of orbitals. Spin delocalization through the pyrrole ring into the carbonyl group then provides a pathway for strong exchange interaction. In conformation W the carbonyl oxygen is further away from the pyrrole ring and spin delocalization can only occur through the meso carbon and phenyl ring. This pathway leads to weak exchange interaction.

The populations of conformations W and S were strongly dependent on porphyrin, axial ligand, and solvent (Table I). For each of the porphyrins in either toluene or chloroform solution the population of conformation W was greater for the 1-methylimidazole complex than for the imidazole complex. The difference between the two axial ligands could be due to the possibility of hydrogen bonding to imidazole but not to 1-methylimidazole or to the steric effect of the additional methyl group. The population of conformation W for II-$(Im)_2^+$ was about the same in ethanol solution as in toluene so hydrogen bonding to imidazole does not appear to be an important factor in determining the population of conformation W. It seems plausible that the steric effect of the methyl group might make the conformation with the carbonyl group near the pyrrole ring less favorable than in the absence of the methyl group and therefore favor a higher population of the W conformation for the 1-methylimidazole complexes than for the imidazole complexes.

The population of conformation W was consistently greater in chloroform solution than in toluene. Spectra in mixtures of chloroform and toluene indicated continuous variation as the composition of the solvent was varied. The population of conformation W for II-$(Im)_2^+$ in acetone and ethanol solution was about the same as in toluene so polarity of the solvent did not appear to be the factor that determined the population of W. Spectra in bromoform were similar to those obtained in chloroform so the variations in the populations of the conformations appeared to be due to a difference between halogenated solvents and other solvents. Morishima et al. reported donor–acceptor interactions between a nitroxyl radical and halocarbons.[39] We have previously reported that interaction with halogenated solvents increased the activation energy for conformational change in a spin-labeled copper porphyrin.[15] Donor–acceptor interaction between the nitroxyl and halogenated solvents or other specific solvation by the halogenated solvents might change the steric requirements of the nitroxyl group thereby favoring the W conformation.

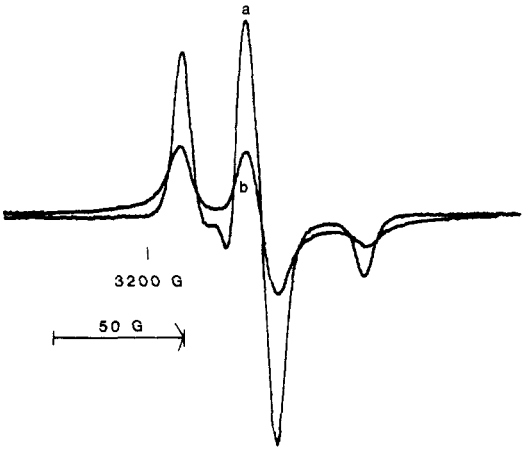

Figure 3. 200-G scans of the X-band (9.10 GHz) EPR spectra at −180 °C of the nitroxyl signals for (A) 1.8 mM II-$(pip)_2$ and (B) the W conformation of 3.1 mM II-$(Im)_2^+$ in toluene/chloroform glasses. The modulations amplitudes were 0.5 (A) and 0.2 G (B) and the microwave powers were 0.02 (A) and 2.0 mW (B). The spectra were replotted to correct for the differences in spectrometer settings and concentrations such that the amplitudes of the signals reflect the decrease in amplitude for II-$(Im)_2^+$ as a result of the broadening due to interaction with the Fe(III). The areas of the two spectra are the same.

Spectra of Conformation W. The spectra of the imidazole and 1-methylimidazole complexes of V–VII and the spectra of the W conformation of the complexes of I–IV had signals at the usual g values for low-spin iron(III) and nitroxyl. Figure 3 compares the spectrum for the nitroxyl in the W conformation of II-$(Im)_2^+$ with the spectrum for II-$(pip)_2$ in which the iron is diamagnetic. The spin–spin interaction in II-$(Im)_2^+$ caused broadening of the nitroxyl signal and resulted in a decrease in the amplitude of the spectrum. The nitroxyl region of the EPR spectra for the W conformations of all of the complexes showed broadening due to the spin–spin interaction. Two models have been proposed to analyze changes in the spectra of nitroxyl radicals in immobilized samples due to a spin–spin interaction that did not cause resolved splitting of the signal.

Kokorin et al. proposed that the ratio d_1/d could be used to determine the distance between a nitroxyl and a paramagnetic transition metal. In his equation d is the height of the central line in the frozen nitroxyl spectrum and d_1 is the height from the maximum for the low-field line to the minimum for the high-field line.[40] This model is based on the assumptions that the interaction is dipolar, that the spin–spin splitting is less than the line width of the spectrum (i.e., $r > \sim 14$ Å), and that the metal T_1 is long relative to the spin–spin splitting.

The values of d_1/d for the W conformations of the complexes of I–VII are given in Table I. In the absence of interaction with a paramagnetic metal, d_1/d was 0.40–0.42 for pyrrolidinyl rings (five-membered saturated nitroxyls) and 0.46–0.48 for piperidinyl rings (six-membered saturated nitroxyls). These values were not strongly dependent on the substitutents on the nitroxyl ring. For all of the spin-labeled iron porphyrins the values of d_1/d were greater than expected in the absence of spin–spin interaction. There was a general trend toward smaller values of d_1/d as the

(38) Walker, F. A. *J. Am. Chem. Soc.* **1980**, *102*, 3254.

(39) Morishima, I.; Inubushi, I.; Yonezawa, T. *J. Am. Chem. Soc.* **1976**, *98*, 3808 and references therein.

(40) Kokorin, A. I.; Zamarayev, K. I.; Grigoryan, G. L.; Ivanov, V. P.; Rozantsev, E. G. *Biofizika* **1972**, *17*, 34 (p 31 in translation).

length of the porphyrin–nitroxyl linkage increased, but the variation was small. In the spin-labeled iron porphyrin samples there were small amounts (1–2%) of nitroxyl impurities that were not attached to an iron porphyrin. These impurities made a negligible contribution to the frozen solution spectrum for most of the complexes. However, for the complexes of I only 7–15% of the sample was in the W conformation so the signal for the impurity had a larger effect on the spectrum than for the other samples in which larger fractions of the sample were in the W conformation. Thus the low values (0.50) for I-$(Im)_2^+$ and I-$(MeIm)_2^+$ may not be accurate. As discussed below, it is likely that the value of T_1 for the iron(III) in these complexes was too short at liquid nitrogen temperature to permit use of this data as a test of Kokorin's model. Kulikov and Likhtenstein also concluded that the T_1 for a low-spin iron(III) porphyrin at liquid nitrogen temperature was too short to permit the use of this model.[41]

In 1970 Leigh proposed a model for the interaction of immobilized nitroxyl radicals with rapidly relaxing transition metals.[42] Two key assumptions of his model are that the correlation time for the electron–electron interaction (usually the metal T_1) was short relative to the electron spin–electron spin splitting of the nitroxyl signal and that the electron–electron interaction was dipolar. Reference 42 has been quoted in the literature as if it stated that the amplitude of the nitroxyl signal was reduced without a change in line shape, although the article states that the amplitude reduction is the result of broadening of the lines and computer simulations emphasized this point.[43] The spectra in Figure 3 clearly show the changes in line width that cause the decrease in the amplitude of the nitroxyl signal.

In Cu(II) and Ag(II) complexes of spin-labeled porphyrins it was observed that exchange interaction was less than 5.0×10^{-4} cm^{-1} for meta- and para-spin-labeled complexes.[18,29] For the ortho-substituted complexes the magnitude of the exchange interaction was strongly solvent-dependent as discussed above. These results suggest that there is little spin-delocalization onto the phenyl rings. In low-spin Fe(III) complexes there is little spin density on the meso carbons[36] which would also contribute to small spin delocalization into the phenyl rings. The angles between the planes of the phenyl rings and the porphyrin plane in metalloporphyrins are typically 65–90° which is not an optimum geometry for spin delocalization from the porphyrin into the phenyl rings.[44] Thus it seems likely that the exchange contribution to the spin–spin interaction in the W conformations was small although it may make some contribution to the changes in the nitroxyl line shape.

Although the value of T_1 for low-spin iron(III) porphyrins is not known, some limits can be estimated. The smallest line widths for the iron signals in the EPR spectra were about 60 G, which indicated that T_2 and T_1 must be $>1 \times 10^{-9}$ s. On the basis of the temperature dependence of the line widths for a low-spin iron(III) heme, T_2 was estimated to be 3×10^{-9} s[11] which would be a lower limit for T_1. Spin–spin splitting was not observed in the spectra of the W conformations for any of the spin-labeled iron(III) porphyrins. In the spectra of the Cu(II) and Ag(II) analogues of II, spin–spin splittings of 20–30 G were observed for the conformations with weak spin–spin interaction.[14,19] CPK molecular models indicate that an iron–nitroxyl distance of about 10 Å, as observed for the Cu(II) analogue, is about the maximum possible for this linkage. It therefore appears likely that the iron(III) T_1 was sufficiently fast to cause collapse of the expected splittings of the magnitude observed for the Cu(II) and Ag(II) complexes. This implies that T_1 must be less than about 4×10^{-9} s. The combined data suggest that T_1 is in the range of (1×10^{-9})–(4×10^{-9}) s.

Since the assumptions of the Leigh model[42] appear to be satisfied for the W conformations, interspin distances were calculated from the amplitude reduction of the nitroxyl signals (Table I) by using values of C taken from the curve in Figure 3 of ref 42 and substitution into eq 2.[42] Equation 2 was obtained from the

$$C = ((4.89 \times 10^{15})T_1)/r^6 \quad (2)$$

equation in ref 42 with the following assumptions, $S = {}^1/_2$, $g = 2$, C is in gauss, r is in angstroms, and $\tau = T_1$. The calculated interspin distances were strongly dependent on the value of T_1 used in the calculation. Table II shows the values of r obtained for two values of T_1 and typical values of the amplitude reduction that were observed for the complexes of I–VII. Ranges of plausible interspin distances estimated for the complexes of I–VII from CPK molecular models are also included in Table II. There is qualitative agreement between the calculated values of r and the distances obtained from the molecular models, although there is substantial uncertainty in both values. Additional data for complexes with different spin states of the metals and different values of T_1 are needed to determine whether these results support the model in ref 42 or whether other models with a dependence on r^{-6} would give similar agreement.

Table II. Estimates of Iron–Nitroxyl Distances in Frozen Solution[a]

porphyrin	rel amp[b]	calcd dist[c] $\tau = 1 \times 10^{-9}$ s	calcd dist[c] $\tau = 3 \times 10^{-9}$ s	CPK models
I, II	0.4	8.6	10.3	7–10
III	0.5	10.0	12.0	8–11
IV	0.6	10.3	12.3	8–11
V–VII	0.8	12.6	15.2	8–16

[a] Distances in angstroms. [b] Typical values of the relative amplitude of the nitroxyl signal (Table I) for the imidazole and methylimidazole adducts of porphyrins I–VII in frozen solution. [c] Interspin distances calculated as in ref 42 from the relative amplitude of the nitroxyl signal for two values of τ.

Table III. EPR Spectra in Fluid Solution

porphyrin	integral[a] toluene[b]	integral[a] $CHCl_3$	line width,[c,d] G
I-$(Im)_2^+$	20	24	7.0 (–40 °C) 8.0 (50 °C)
I-$(MeIm)_2^+$	38	35	6.5 (–40 °C) 12.0 (50 °C)
II-$(Im)_2^+$	93	100	35.0 (–40 °C) 24.0 (50 °C)
II-$(MeIm)_2^+$	95	90	25.0 (–40 °C) 7.5 (50 °C)
III-$(Im)_2^+$	75	100	5.0 (–40 °C) 20.0 (50 °C)
III-$(MeIm)_2^+$	25	90	4.0 (–40 °C) 20.0 (50 °C)
IV-$(Im)_2^+$	85	95	7.0 (–40 °C) 20.0 (50 °C)
IV-$(MeIm)_2^+$	15	70	5.0 (–40 °C) 20.0 (50 °C)
V-$(Im)_2^+$	95	100	2.8 (–40 °C) 3.4 (50 °C)
V-$(MeIm)_2^+$	100	100	2.4 (–40 °C) 2.1 (50 °C)
VI-$(Im)_2^+$	75	90	2.4 (–40 °C) 2.2 (+50 °C)
VI-$(MeIm)_2^+$	50	100	2.5 (–40 °C) 1.8 (+50 °C)
VII-$(Im)_2^+$	50	95	2.9 (–40 °C) 9.0 (+50 °C)
VII-$(MeIm)_2^+$	40	60	3.0 (–40 °C) 15. (+50 °C)

[a] Integrated intensity of the nitroxyl signal at room temperature for a 1000-G scan, expressed as a percent of that observed for a standard at the same concentration. Uncertainties are ±5%. [b] 9:1 toluene/$CHCl_3$ was used for the imidazole adducts. [c] Line width of the nitroxyl $m_I = 0$ line in spectra obtained at the temperature indicated in parentheses. Due to the presence of low concentrations of noninteracting nitroxyl signals with narrow line widths, uncertainties in the line widths ranged from ±0.2 G at 2.0 G to ±5 G at 35 G. [d] Degassed samples in toluene solution.

(41) Kulikov, A. V.; Likhtenstein, G. I. *Adv. Mol. Relax. Interact. Processes* **1977**, *10*, 47.
(42) Leigh, J. S., Jr. *J. Chem. Phys.* **1970**, *52*, 2608.
(43) Eaton, S. S.; Law, M. L.; Peterson, J.; Eaton, G. R.; Greenslade, D. J. *J. Magn. Reson.* **1979**, *33*, 135.
(44) Hoard, J. L. *Ann. N. Y. Acad Sci.* **1973**, *206*, 18.

EPR Spectra in Fluid Solution. The EPR spectra of the nitroxyl signals for the imidazole and 1-methylimidazole complexes of I–VII in fluid solution at room temperature had line widths between 2 and 30 G. Integration of 1000-G scans of the spectra indicated that for most of the complexes in toluene solution, part of the nitroxyl signal was sufficiently broad that it did not contribute to the integral (Table III). A larger fraction of the nitroxyl signal was observed in chloroform solution than in toluene solution. This pattern was similar to that observed in frozen solution. It was therefore proposed that both W and S conformations of the complexes of I–IV were present in fluid solution, that the rate of interconversion of the two conformations was slow on the EPR time scale, and that the spectra of the S conformations were too broad at room temperature to permit detection in the presence of the sharper signals from the W conformation. For the imidazole complexes of I–IV and the 1-methylimidazole complexes of I and II the population of the W conformation was greater in fluid solution than in frozen solution. Molecular motion may tend to displace the carbonyl group from the special orientation near the pyrrole ring required for significant exchange interaction. For the 1-methylimidazole complexes of III and IV, less of the nitroxyl signal was observed at room temperature than in frozen solution. The preferred conformations of the 1-methylimidazole at room temperature in these complexes may cause less steric interference with the amide group of the S conformation than in frozen solution.

Although 100% of the nitroxyl signal in the complexes of V–VII was observed for the W conformation in frozen solution, some of the nitroxyl signal in these complexes was not observed at room temperature. These differences suggest that a greater variety of conformations are present in fluid solution than in frozen solution and that in some of the conformations that are present in fluid solution there is stronger spin–spin interaction between the iron and the nitroxyl than was observed in frozen solution. The amount of the signal that was not observed in toluene solution increased as the length of the linkage between the phenyl ring and the nitroxyl was increased. Thus the longer ether linkages provided greater opportunity for stronger spin–spin interaction than the shorter ether linkages. This suggests that the longer chains can fold in such a way as to put the amide linkage or the nitroxyl ring in a position that permits overlap with other portions of the molecule that have substantial unpaired electron spin density.

The spectra of the nitroxyl signals for the imidazole and 1-methylimidazole complexes of I–VII in toluene solution were studied as a function of temperature from −40 to +50 °C. The line widths of the nitroxyl signals exhibited different dependence on temperature for different porphyrins (Table III). There was little change in line width as a function of temperature for I-$(Im)_2^+$ and for the complexes of V and VI. For I-$(MeIm)_2^+$ and the complexes of III, IV, and VII the line widths increased with increasing temperature. For the complexes of II the line widths decreased with increasing temperature.

Several factors could contribute to narrowing of the lines with increasing temperature. The broadening of the high-field lines in the nitroxyl spectra at −40 °C indicated slowing of the molecular tumbling. Thus incomplete motional averaging of the anisotropic g and A tensors and of the anisotropic dipolar spin–spin interaction contributes to the line widths at this tempeature. This contribution to the line width decreases with increasing temperature due to increased rates of tumbling. At room temperature the T_1 for iron(III) in FeTTP$(Im)_2^+$ was estimated to be $\sim 8 \times 10^{-12}$ s on the basis of the line widths in the NMR spectrum.[45] A somewhat longer value of T_1 would be expected at −40 °C than at room temperature. Decreases in T_1 with increasing temperature could cause narrowing of the nitroxyl signal if the broadening due to the spin–spin interaction was not fully collapsed by a T_1 of this magnitude. Both of these factors could influence the line widths of the nitroxyl signals in all of the complexes. However, for some of the complexes these effects apparently were overwhelmed by other factors that contribute to increased line widths at higher temperatures.

Several factors could contribute to increased line widths at higher temperatures. The increased frequency of collisions between paramagnetic centers at higher temperatures causes line broadening. However, since the solutions were about 1 mM this contribution to the line widths would be only a few gauss, even at +50 °C.

The nitroxyl spectrum at room temperature is assigned to the W conformation. If the rate of interconversion between the W and S conformations of I–IV became sufficiently fast on the EPR time scale, the spectrum of the W conformation would be broadened. In the fluid solution EPR spectra of the Cu(II) and Ag(II) analogues of II there was rapid exchange between the conformations that gave strong and weak spin–spin interaction.[18,29] Although the barriers to conformational interconversion are probably different for the 6-coordinate complexes of Fe(III) and the 4-coordinate complexes of Cu(II) and Ag(II), the onset of interconversion of W and S conformations of the complexes of I–IV on the EPR time scale might contribute to increasing line widths at higher temperatures. The magnitude of the broadening would be determined by the steric hindrance to conformational changes and so might vary substantially between the complexes.

NMR studies of Fe(P)$(Im)_2^+$ and analogous complexes with substituted imidazoles have found that the rate of exchange between free 1-methylimidazole and 1-methylimidazole coordinated to iron(III) tetratolylporphyrin at room temperature was about 80 s^{-1}.[46,47] The rate of dissociation of 1-methylbenzimidazole was about 4×10^4 times faster than the rate of dissociation of 1-methylimidazole, which was attributed to steric effects on the binding.[47] Substantial dissociation to form Fe(P)$(Im)^+Cl$ was noted at temperatures greater than about 50 °C and exchange was observed between Fe(P)$(Im)_2^+$ and Fe(P)$(Im)^+Cl^-$.[47] When a sample of II-$(Im)_2^+$ was heated above 50 °C the color changed from red (characteristic of 6-coordinate low-spin complexes) to yellow. Thus the dissociation of imidazole from the spin-labeled iron porphyrins was significant at elevated temperatures. If the broadening of the EPR spectra at room temperature ($\sim$10 G) is attributed to exchange broadening, the rate of dissociation would be about 8×10^7 s^{-1}, which is about 10^6 times faster than the rates obtained for FeTTP$(MeIm)_2^+$ and about an order of magnitude faster than for 1-methylbenzimidazole. The bulky ortho substituents on I–VII could have substantial effects on the rate of exchange but the calculated rates seem unreasonably fast for the observed broadening of the nitroxyl EPR spectra to be due to exchange between Fe(P)$(Im)_2^+$ and Fe(P)$(Im)^+$.

In spin-labeled nickel(II) complexes with flexible linkages between the nickel and the nitroxyl, the line widths of the nitroxyl signal increased with increasing temperature.[48] The broadening was attributed to motion of the linkage between the nickel and the nitroxyl that permitted occasional close approach of the nitroxyl to regions of the molecule with high unpaired spin density.

Of the options discussed above, increasing rates of interconversion between W and S conformations with increasing temperature appears to be the most plausible explanation of the broadening of the nitroxyl signals in some of the complexes as a function of temperature, though other dynamic processes cannot readily be excluded.

Interpretation of Spectra of Spin-Labeled Complexes of Cytochrome P450. When nitroxyl radical VIII was coordinated to cytochrome P450, the EPR spectra in frozen solution showed spin–spin splitting of the iron and nitroxyl signals.[10,12] It was assumed that the splitting was due to dipolar interaction and the splitting of the iron signals was analyzed to obtain an interspin distance of 5.7 Å.[12] The iron unpaired electron is in the d_{xz},d_{yz} pair which has the appropriate symmetry to interact with the p-orbital on the pyridine nitrogen. The symmetry of this interaction is analogous to that for pyridine coordinated to vanadyl bis(hexafluoroacetylacetonate), VO$(hfac)_2$.[49] Therefore the

(45) LaMar, G. N.; Walker, F. A. *J. Am. Chem. Soc.* **1973**, *95*, 1782.

(46) LaMar, G. N.; Walker, F. A. *J. Am. Chem. Soc.* **1972**, *94*, 8607.

(47) Satterlee, J. D.; LaMar, G. N.; Bold, T. J. *J. Am. Chem. Soc.* **1977**, *99*, 1088.

(48) Smith, P. H.; Eaton, G. R.; Eaton, S. S. *J. Am. Chem. Soc.* **1984**, *196*, 1986.

exchange interaction would be expected to be similar if the same ligand were coordinated to $VO(hfac)_2$ or to the heme in cytochrome P450. When spin-labeled pyridine IX was coordinated to $VO(hfac)_2$ the value of the exchange coupling constant J was 7×10^{-4} cm^{-1}.[49] Since the values of J for the $VO(hfac)_2$ complexes were smaller when the spin labeled substituent was on the 3-position of the pyridine than for the 4-substituted analogue, weaker exchange would be expected for complexes of VIII than of IX.

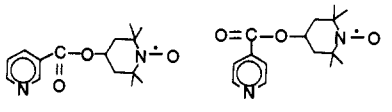

VIII IX

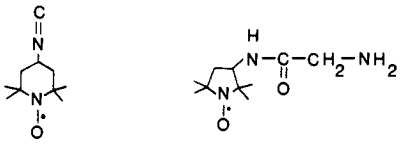

X XI

Therefore the assumption that exchange interaction was negligible for the cytochrome P450 complex of VIII was reasonable.

In ref 5 and 6 it was reported that when isocyanide X coordinated to cytochrome P450 the complex had g values of 2.19, 2.08, and 1.97. These g values are approximately the averages of those obtained for cytochrome P450 bonded to long-chain isocyandes (2.45, 2.30, 1.91) and nitroxyl radicals ($g \sim 2$) which suggests that the spectrum was due to strong exchange interaction between the unpaired electrons on the iron and the nitroxyl. Simulated spectra indicated that $|J| \geq 0.4$ cm^{-1} would be required to give these average g values. Such a large value of J is reasonable for an isocyanide bridging between the metal and the nitroxyl ring.

When nitroxyl XI was coordinated to cytochrome P450 new signals were reported at $g = 2.047$ and 2.101.[6,13] The spectrum shown in Figure 5a of ref 6 also indicated new signals at $g \sim 1.90$ and 1.88. These features were reproduced by simulated spectra with $r = 7$ Å, $\epsilon = 25^0$, and $J = -0.03$ cm^{-1} (the definition of ϵ is given in ref 14). CPK molecular models indicate that the values of r and ϵ are consistent with plausible conformations of the ligand. For this magnitude of J and the large g-value differences between the iron and nitroxyl unpaired electrons, there is little mixing of the iron and nitroxyl wavefunctions. Thus the effect of the exchange interaction on the nitroxyl signal is nearly isotropic, despite the anisotropy in the iron g values. The splitting into signals at 2.047 and 2.101 is due to the contribution from the anisotropic dipolar interaction and thus is quite sensitive to the interspin distance. The iron signals from the spin-labeled complex were not resolved due to overlap with the spectrum of cytochrome P450 that was not coordinated to the spin label. Attempts to simulate the spectrum without exchange interaction were unsuccessful.

The spectra in the literature for spin labels coordinated to the heme in cytochrome P450 provide examples of interaction dominated by exchange interaction (ligand X) or dipolar interaction (ligand VIII) and an example where the two contributions are of comparable magnitude (ligand XI). They provide a good example of the need to consider both contributions when analyzing metal-nitroxyl interactions.

Acknowledgment. This work was supported in part by NIH Grant GM21156. S.S.E. thanks NSF for a Visiting Professorship for Women, 1984. We thank Professor Belford for a copy of his fourth-order frequency shift perturbation routine and for helpful discussions concerning this method. Mass spectral determinations were performed by the Midwest Center for Mass Spectrometry, a National Science Foundation Regional Instrumentation Facility (Grant CHE 8211164).

(49) Sawant, B. M.; Shroyer, A. L. W.; Eaton, G. R.; Eaton, S. S. *Inorg. Chem.* **1982**, *21*, 1093.

Deuterium Isotope Effects on Nuclear Shielding. Directional Effects and Nonadditivity in Acyl Derivatives†

Poul Erik Hansen,‡ Flemming M. Nicolaisen,§ and Kjeld Schaumburg*§

Contribution from the Institute I, Roskilde University Centre, DK-4000 Roskilde, Denmark, and the Department of Chemical Physics, The H.C. Ørsted Institute, University of Copenhagen, Universitetsparken 5, DK-2100 Copenhagen Ø., Denmark. *Received April 8, 1985*

Abstract: Deuterium isotope effects on the ^{19}F and ^{13}C nuclear shieldings have been investigated in acyl derivatives. A nonadditivity of the $^3\Delta F(D)$ of acetyl fluoride has been experimentally established and related primarily to nonuniform rotamer distributions of the mono- and dideuterated isotopomers. The $^3\Delta F(D)$'s show furthermore a distinct orientational dependence. The isotope effects for the configurations where the nuclei in question are in a trans position are positive and those in which they are gauche are negative. The $^2\Delta CO(D)$'s are negative and additive in all the investigated cases. The observed isotope effects are discussed in general in terms of substituent and vibrational effects.

The interest in isotope effects on nuclear shielding has gradually increased due to the advent of high-field NMR spectrometers.[1] They have with their high sensitivity made possible the observation of isotope effects in many unenriched samples and simultaneously extended the possibility of observing isotope effects due to long-range effects. It has become apparent that many of the observed effects are of use both for spectral interpretation and for structural elucidation.

The origin of the isotope effect is entirely vibrational. In spite of the advances in vibrational analysis and force constant calculations currently taking place, no accurate interdependence of the long-range isotope effects on chemical shift has been established. The observation of a negative $^2\Delta CO(D)$ in acetone[2] as well as

† Presented in part at the VIth International Meeting on NMR, Edinburgh, July 1983.

‡ Roskilde University Centre.

§ University of Copenhagen.

(1) Hansen, P. E. *Annu. Rep. NMR Spectrosc.* **1983**, *15*, 105.

(2) Maciel, G. E.; Ellis, P. D.; Hoper, D. C. *J. Phys. Chem.* **1967**, *71*, 2161.

0002-7863/86/1508-0625$01.50/0